

Review of Jets in a Cross Flow-Experimental and Numerical Approach

Sharmishtha Chakraborty, Utpal Bhattacharjee

Abstract: A literature review was performed on experimental and numerical studies of open channel and open channel with cross flow. Open channel flow was studied because it was used to obtain the flow behaviour without any impingement. Open channel with a jet flow was studied to see the mixing behaviour of fluids in a cross flow situation. In addition, it has been used to validate the numerical model with experimental data. Both turbulent and laminar jets in cross flow were studied so that basic insight into such structures can be gained and by that, correlation of jet trajectories can be understood in both the cases. Finally, in this section some basics of computational fluid dynamics (CFD) and earlier work of the transverse jet by the CFD analysis have been discussed. This can provide insight on the modelling procedures and techniques to obtain accurate results.

Keywords: Open Channel, Cross Flow, Jet Trajectories, Transverse Jet, CFD.

I. INTRODUCTION

The characteristics of flow propagation under water are always of interest to scientists and researchers in the field of hydraulics and river management [1-4]. The flow patterns of water waves and various characteristics like velocity, shear stress and turbulence have been studied by several researchers with different configurations [3, 5, 6]. Experiments and investigations of mixing and dispersion of turbulent jets issued from a nozzle have industrial applications in wastewater disposal and in river management. The mixing and dispersion patterns of a jet in a crossflow can also be applicable to discharging pollutants into the atmosphere. Previous research into hydraulics and environmental engineering has included experiments of open channel and crossflows. It is almost impossible to reference all of them. However, an excellent and comprehensive review of the past work of jet in crossflow has been reported by Margason [7]. In the past studies, researchers have considered many different aspects of the flow in case of jet in crossflow. For example, they have studied velocity and vorticity fields, the jet trajectory and the propagation of the large scale flow structures [8-12], concentration, mixing and passive scalar fields [13-15], the effect of temperature on jet structure [16]. To investigate additional flow properties, numerical simulations have been used extensively in recent years [17-19].

The main features of the jet in crossflow have been explained in detail by the analysis of experimental studies followed by the numerical studies. Numerical studies provide useful explanations of complex phenomena that can be found in experimental studies. Previous experiments and numerical simulations related to jet in crossflow are summarised below.

II. EXPERIMENTAL STUDIES OF OPEN CHANNEL FLOW

Experiments and analysis of open channel focusing on different parameters like velocity distribution, turbulence characteristics, wall and bed shear stresses, effect of secondary currents both in narrow and wide-open channel have been done previously. Some of those studies have been discussed here to understand the characteristics of the fully developed turbulent flow without any jet. Experiments of open channel has been done by Steffler et al [20].

Velocity and turbulence measurements of subcritical flow with three aspect ratios in smooth rectangular open channel have been obtained and validated with theoretical data. To measure the longitudinal and vertical velocity components in two-dimensional fully developed flow Nezu and Rodi [21] used a laser Doppler anemometer. With a smooth bed near the wall, the velocity profile well agrees the law of the wall and they have re-examined the fact in case of open channel. They have compared the data with pipe flow and close channel flow. Their data of velocity and turbulence intensities are still used by the researchers as the basis for open channel research. Sharma et al [1], Nezu and Rodi [2] and Nezu [22] have found that in open channels, the mean longitudinal velocity distribution in 3D flows is much more complicated than for 2D flows, especially in the outer region. Outer region was defined as $y/y_{\max} > 0.2$, where y_{\max} is the distance from the position of maximum velocity to the channel bed. They have revealed the peculiar phenomena called 'velocity-dip'; i.e.; the maximum velocity appears not at the free surface, rather just below it. Velocity vectors of secondary currents in a narrow open channel measured by Nezu and Rodi [2] have been shown in Fig 1. They have found two types of vortex, one near the free surface and another near the bed. These vortex are called 'free surface vortex' and 'bottom vortex' respectively. The free surface vortex is much stronger than the bottom vortex. The free surface vortex transports momentum and energy from the side wall toward the channel centre near the free surface. As momentum is transported from the free surface to the mid-depth, the strong down flow (that occurs at the channel centre) causes the velocity dip.

Manuscript published on 30 December 2017.

* Correspondence Author (s)

Sharmishtha Chakraborty*, Department of Engineering, Edith Cowan University, Western Australia-6027.

Utpal Bhattacharjee, Repair and Production Division-1, Bangladesh Water Development Board, Narayanganj-1400, Bangladesh.

© The Authors. Published by Blue Eyes Intelligence Engineering and Sciences Publication (BEIESP). This is an open access article under the CC-BY-NC-ND license <http://creativecommons.org/licenses/by-nc-nd/4.0/>

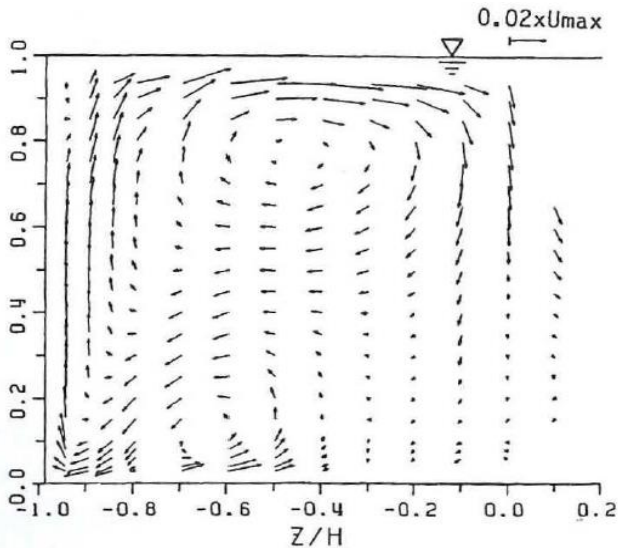


Fig 1 Vector Description of Secondary Currents in Open Channel [2]

Three dimensional turbulent structure in straight open channel and the effect of secondary currents have been studied by Tominaga et al [3]. They have compared their data with closed channel and found that secondary current motions are quite different in both the cases. Studies of shear stress in open channel have been done by Yang and Lim [5], Guo and Julien [23] and Blanckaert et al [24]. A comparison of six different methods of determination of boundary shear stress in open channel has been studied by Khodashenas et al [6]. They found that with some empirical correction factors, Guo and Julien method best predicts the mean wall and bed shear stress in smooth open channel.

Turbulent velocity profiles in fully developed open channel flow has been investigated by Bonakdari et al [4]. With presence of anisotropic turbulence effects in narrow open channel, the determination of velocity profile is difficult. Because in this type of flow, Prandtl's second type of secondary flow appears in the cross-section and causes the dip phenomena, that is, maximum velocity appears just below the free surface. In the inner region with a smooth wall, in general, the value of dimensionless velocity and the value of the dimensionless wall distance are same. The inner region is much smaller than the outer region. Of the total boundary layer, only 10-20% represent the thickness of inner region [25]. In this region, the generation of turbulent kinetic energy is higher than the rate of dissipation. The inner region is divided in a viscous sub-layer, adjacent to the wall, an intermediate area of transition (buffer region), and a fully turbulent region. They [4] have found that the well-established log-law is suitable for inner region of turbulent boundary layer but not appropriate for velocity distribution for outer region in narrow open channels.

III. EXPERIMENTAL STUDIES OF JET IN CROSSFLOW

Studies of jets in a crossflow have different focusing parameters. Investigation of jet trajectory, jet cross-section, counter-rotating vortex pair (CVP), horseshoe and wake vortices, scalar transport and mixing were main considerations for the previous researchers. In this section,

the experimental outcomes of jets in a crossflow of previous research have been discussed.

Andreopoulos and Rodi [9] measured the mean and fluctuating velocity components for jet in crossflow with different velocity ratios (0.5, 1.0 and 2.0) by using a three sensor hot-wire probe. The corresponding Reynolds numbers were 20500, 41000 and 82000. At small velocity ratios (r , jet to crossflow velocity), the jet bends over abruptly by the crossflow, in the case of $r=0.5$. At higher r values, the jet penetrates further into the cross-stream, and the bending over takes place more gradually (Fig 2 and Fig 3). The shear stress controlling the lateral spreading of the jet was found to be generated mainly by the two velocity gradients (velocity gradients along z -axis and y -axis). They established that the shear stress which acts to damp the secondary vortex motion, was found to be closely related to the velocity gradients. Towards downstream, the uniform kinetic energy distribution suggested less production of turbulent kinetic energy were diffused by the turbulent motion towards the wall. They found that the lower the velocity ratio the higher the distortion of the jet flow by the crossflow.

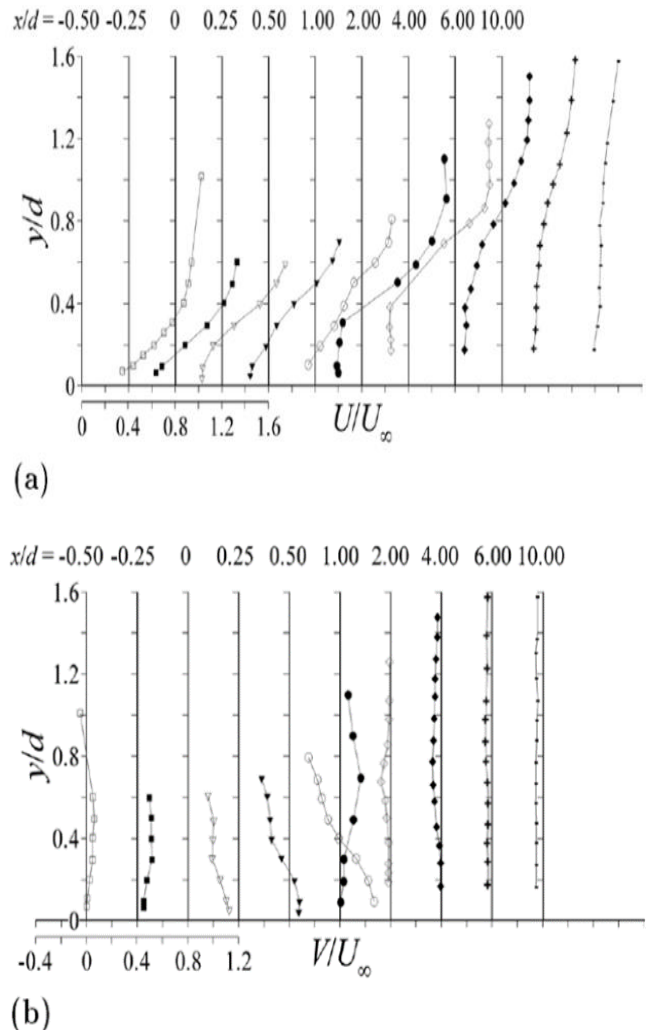


Fig 0 (a) Mean u-velocity profiles at the plane of symmetry $z/d=0$, $r=0.5$ and (b) Mean v-velocity profiles at the plane of symmetry $z/d=0$ and $r=0.5$ [9]

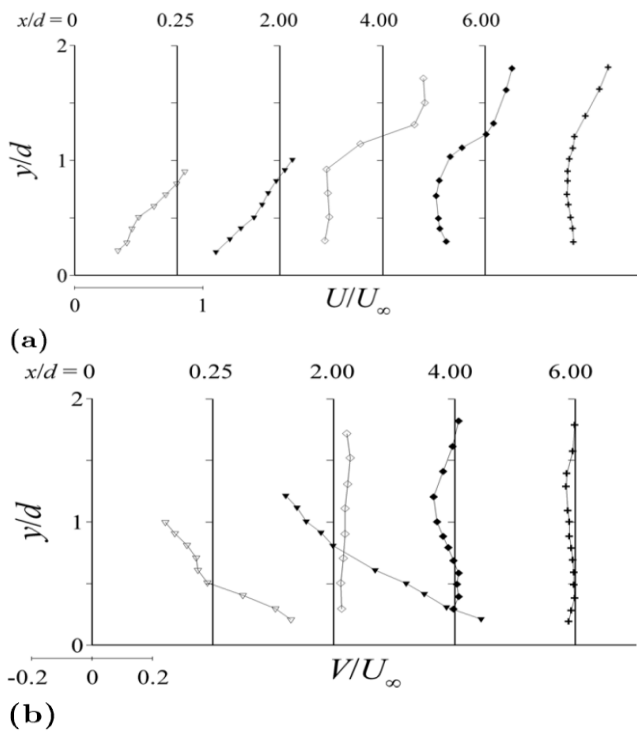


Fig 3 (a) Mean u-velocity profiles at the plane of symmetry $z/d=0$ and $r=1$ and (b) Mean v-velocity profiles at the plane of symmetry $z/d=0$ and $r=1$ [9]

The turbulence measurements (Fig 4) have shown that the turbulent kinetic energy and the primary shear stress are closely related to the velocity gradient. They found that the velocity gradient in lateral direction significantly contributes to the productions of kinetic energy and shear stress. For low values of r , the kinetic-energy balance at the exit was rather unusual as production by all velocity gradients was significant.

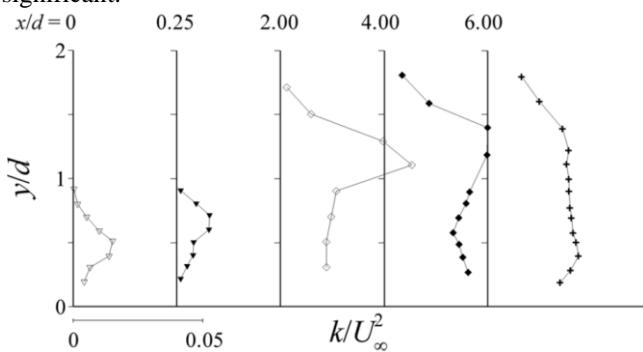


Fig 4 Turbulent Kinetic Energy Profiles at the Plane of Symmetry $z/d=0$ and $r=1$ [9]

Experiments with three-dimensional single and multiple free jets were performed by Pani and Dash [26] to get the distribution of momentum flux and stream-wise mean velocity. They concentrated on the maximum velocity decay along the axis of the jet exit. Flow and turbulence characteristics of round jets in crossflow were investigated by Sharif and Pletcher [16], Fric and Roshko [10] and Kelso *et al* [11]. In all those cases, the jet was inserted from the bottom of the channel and velocity ratios were varied to see the effect of these changes into the flow. Vortical structure in the wake of a transverse jet was investigated by Fric and Roshko [10]. They considered the range of velocity ratio from 2 to 10 and crossflow Reynolds number was from 3800 to 11400. Their observation was that, the wake

vorticity comes from the crossflow boundary layer and not from the shed of the jet. This is due to the adverse pressure gradient imposed by the jet. The origin and formation of vortices in the wake are fundamentally different from the well-known vortex shedding phenomena of solid bluff bodies. They found that the origins of wake vortices are in the laminar boundary layer of the wall. Figure 5 shows the jet shear-layer vortices at the perimeter of the bending jet, the developing counter-rotating vortex pair, horseshoe vortices on the wall, and wake vortices extending from the wall of the jet.

In low velocity ratio, the similar trend for turbulent kinetic energy was also observed by Andreopoulos and Rodi [9]. Kelso *et al* [11] investigated flow structures in both water and wind tunnel. Different vortex structures were observed by hot-wire measurement and they interpreted the major roll-up process of the jet shear layer. They described the large-scale vortex roll-up (ring-like) and showed reorientation of shear layer vorticity that forms the counter rotating vortex pair (CVP). This interpretation agrees well with the mechanism proposed by Andreopolpus [27]. They concluded that from low to high velocity ratio, the flow structure changes from wake-like to jet-like (Fig 6) and this confirms the results of Fric and Rosko [10].

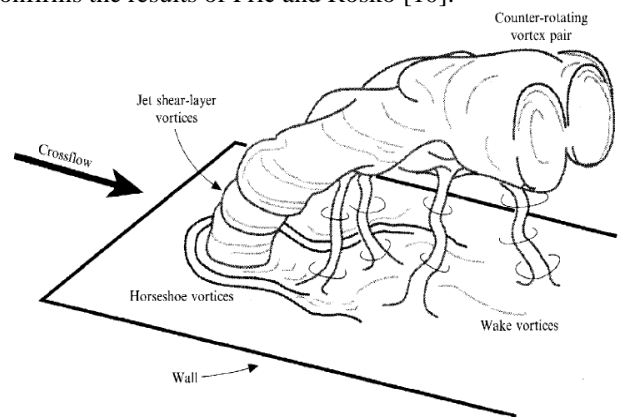


Fig 5 Cartoon Depicting Four Types of Vortical Structure Associated with the Transverse Jet Near Field [10]

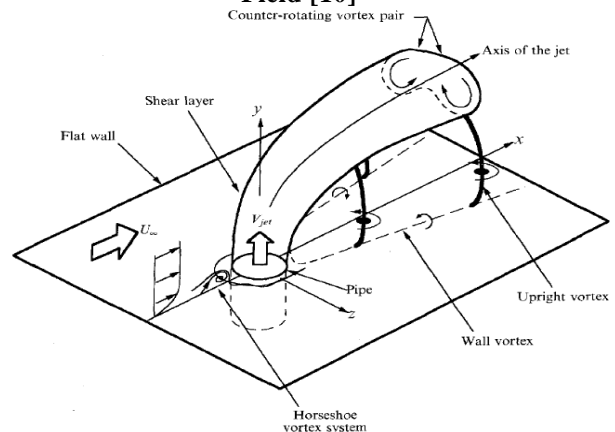


Fig 6 Schematic Diagram Showing Many Vortex Systems of a Jet in Crossflow. Wall Vortices or Upright Vortices Are Considered to be Part of the wake Region [27]

Morton and Ibbeston [28] studied the entrainment of crossflow and explained the mixing mechanism. This experiment also proves that the wake vortices are generated from the crossflow boundary layer. Lim and New [29] concentrated their focus on the large scale vortex structures. After their experiment, Lim and New proposed a model which explains the correlation of shear layer vortex and CVP. Their results show that after the jet emerged from the nozzle, its edges folded up and form CVP. This observation is also consistent with the experimental findings of Kelso et al [11].

Dynamics of near field of strong jets in crossflow were studied by Coelho and Hunt [30]. They found that jet dynamics are controlled by the entrainment and transport of transverse components of vorticity. In addition, the diffusion of vorticity into the wake is weak and so the jet does not work as a solid body, and it is comparable with the findings of Fric and Rosko [10]. Instability in the shear layer vortices were investigated by many [10, 12, 31] and thought to results from a Kelvin-Helmholtz instability near the jet exit [10, 11]. Unsteady behaviour of jets had been studied by Blanchard et al [32]. An experimental investigation was carried out by using several nonintrusive optical methods (Laser Induced Fluorescence, Particle Streak Velocimetry). Their study found that longitudinal structures must be taken into account in the mechanism of stability arising from the meeting of a jet and a crossflow with a low Reynolds number ($Re < 1000$). Contrary to previous research [10, 11], Balnchard et al [32] argued that the near field instability are not the Kelvin-Helmholtz type but they are elliptical in nature.

Ozcan and Larsen [33] studied jet entrainment in the low speed wind tunnel by LDV measurements. Based on their velocity data, the authors speculated that the jet flow fluid enters the plane of symmetry about 2 jet diameters downstream of jet axis, and then it disperses in all directions. This statement is supported by Lim et al [29] who did their flow visualization studies.

Roth et al [34] examined the evaluation of Navier-Stokes prediction of a subsonic jet in crossflow. They investigated the entire picture of flow field considering vortex pair in air by jet. They found a contra rotating vortex pair that divides the jet centreline or vortex trajectory. They considered a normal subsonic jet exhausting perpendicularly through a large flat plat into a subsonic crossflow. They emphasised on characterizing the contra rotating vortex pair for evaluating the fluid mechanics of a jet in crossflow.

Eroglu and Breidenthal [35] investigated the effects of exponential acceleration on penetration and mixing characteristics of jet in crossflow. Figure 7 shows sketch and an internal, streamwise LIF picture of the round jet in a crossflow. For increasing the exponential acceleration of flow, both the injection speed and the nozzle width of the jet were increased in the downstream direction of the cross flow. They found that by imposing an external time scale on the large-scale structure of a jet in a crossflow, it significantly alters its entrainment and mixing characteristics. In their study, they used an acceleration parameter which can be defined as the ratio of the two timescales. One is the revolution time of the longitudinal vortex pair and other is the e -folding time of the

acceleration. e -folding is the time interval in which an exponentially growing quantity increases by a factor of e ; it is the base- e analog of doubling time [36]. From their experimental result, they claimed that like jet to crossflow momentum ratio, acceleration is a valuable tool to control mixing and penetration of a jet in crossflow.

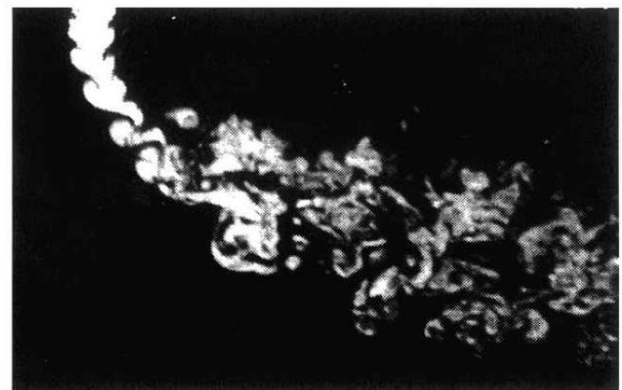
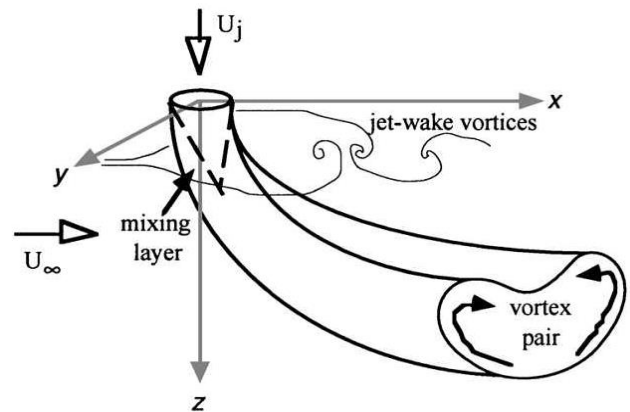


Fig 7 Sketch and an Internal, Stream Wise LIF Picture of the Round Jet in a Crossflow [35]

Experimental study of a jet in a crossflow at low Reynolds number was studied by Camussi et al [37] with a gravity driven water tunnel. They considered the range of velocity ratio from 1.5 to 4.5 and velocity ratio $r \cong 3$ was considered as a transitional value. $r < 3$ and $r > 3$ was considered as low and high velocity ratio, respectively. By keeping the free stream velocity constant, they changed the velocity ratio only by changing the jet velocity. PIV was used for flow visualization. They focused the effects of velocity ratio on the formation and evaluation of large scale vortices. They observed two different flow characteristics at low and high velocity ratio. They found that jet Reynolds number plays an important role on the destabilization mechanisms which lead to the formation of the jet shear-layer structures. However, as the jet flow was laminar, so turbulent characteristics were not studied. Velocity characteristics of crossflow have been measured by Barata and Durao [38] with a confined crossflow by Laser Doppler Velocimeter (LDV). Flow produced by a single jet discharged through the upper wall of a rectangular water channel of large cross-section (0.5mx0.1m) at right angles to the channel was measured.

Their aim was to characterise the influence of the jet to crossflow velocity ratio on the structure of the ground vortex. They used velocity ratio (jet to crossflow ratio) of 30, 45 and 73 respectively in their experiment and three different Reynolds numbers of 60000, 84000 and 120000, respectively. They found that with low velocity ratio, the deflected jet becomes almost parallel to the ground plate. The upstream wall jet interacts with the crossflow and forms a vortex close to the ground plate which wraps around the impinging jet like a scarf. As a result, two stream wise counter-rotating vortices develop side to side and decay further down-stream of impinging zone (Fig 8). Figure 9 shows the ground vortex caused by the interaction of the crossflow with the upstream wall jet. As the velocity ratio was large, the jet flow created a scarf vortex, however, for the range of low velocity, the flow structure might be different.

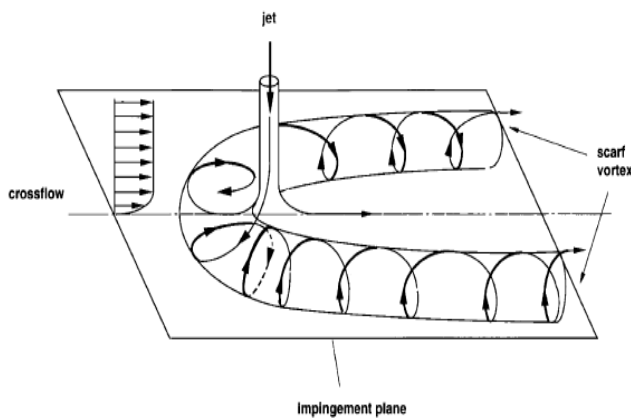


Fig 8 Jet Impinging on a Flat Surface Through a Low-Velocity Crossflow [39]

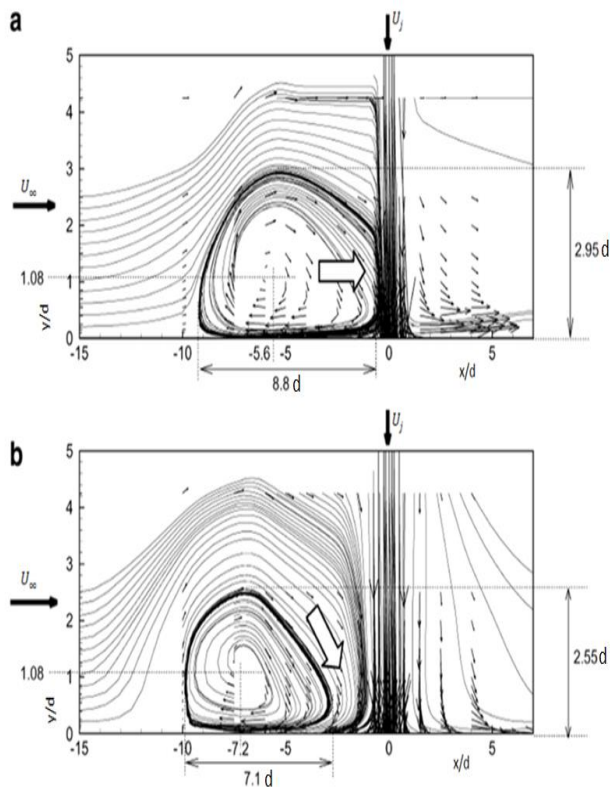


Fig 9 Measured Mean Velocity Characteristics in The Vertical Plane of Symmetry for Two Different Jet To Crossflow Velocity Ratios: (a) r=30 and (b) r=45 [39]

The flow structure and distributions of mean velocity, vorticity and turbulence intensity were measured by Gopalan et al [40] with a closed-loop water tunnel. They used a PIV system and considered velocity ratios from 0.5 to 2.5. They found that there are two distinctly different structures of a jet in crossflow at high Reynolds number. At low velocity ratio, the vorticity in the forward side of the jet is cancelled due to mixing with crossflow boundary layer. At high velocity ratio, the jet vorticity is advected away from the wall and remains mostly confined to the jet. However, they did not mention the effect of a free surface in the case of a low velocity ratio.

Su and Mungal [14] measured the planar scalar mixing and two-dimensional velocity fields in a jet in crossflow with jet to crossflow velocity ratio of $r=5.7$ and Reynolds number [41] at jet exit $Re_j=5000$ with planar Laser-Induced Fluorescence (PLIF) and PIV. (Reynolds number is a non-dimensional quantity, $Re = UL/\nu$ [41]), Figure 10 shows the boundary contours of the concentration field in the centre-plane for varying z-positions. They found that the deepest penetration on the outer boundary occurs in the centre-plane and a shallower penetration for increasing off-centre positions of z. The curves in the figure represent the loci of points where the local mean scalar value is 20% of the maximum value in the centre-plane.

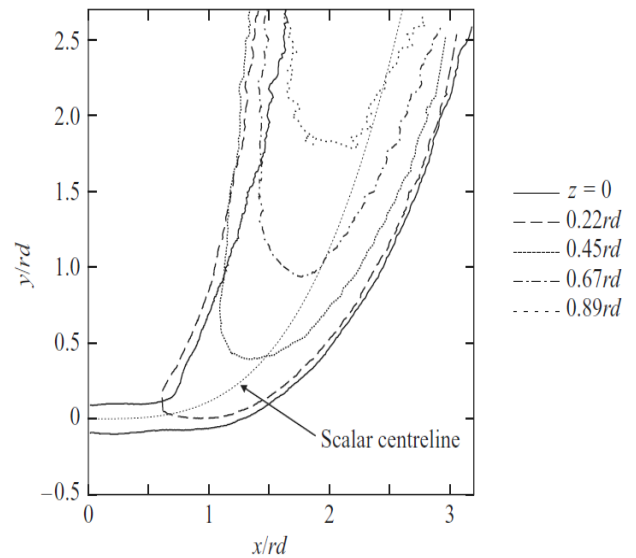


Fig 10 Boundary Contour for the Mean Scalar Fields [14]

In another experiment, they provided a comprehensive view of the velocity and scalar fields in the developing region of the flow. They focused on the fields of fluctuating quantities including the scalar variance C'^2 , the scalar flux components $u'C'$, the turbulence normal stresses, u'^2 and v'^2 and the turbulent shear stress $u'v'$. The estimated finest length scales in the velocity and scalar fields were given by λ_v and λ_d , respectively. The grid resolution of the scalar field images was Δx_c , and the grid resolution of the velocity fields was given by Δx_u . Table 1 shows the result of this study.

Table 1 Outer Scale Parameters And Resolution Estimates

s/rd	U (m/s)	δ (m)	Re_δ	λ_v (μm)	λ_d (μm)	Δx_c (μm)	Δx_u (μm)
1	11.3	0.019	14100	220	180	175	230
2	4.0	0.041	10800	580	480	175	310
3	3.0	0.046	9100	740	610	175	420
3.5	2.6	0.052	8900	850	700	175	420

Where s is a quantity, in downstream coordinate defined by local maxima in the averaged velocity magnitude field, δ is a measure of local mean flow width, u is the mean velocity of the flow. Re_δ is Reynolds number in terms of δ and u .

They found that the intensity of mixing was initially higher on the jet windward side, but eventually becomes higher on the wake side. The scalar flux results also indicate that cross-stream turbulent transport is more significant than the streamwise transport, particularly in the near field of the flow. However, there is no evidence about the near field

scalar flux in the case of a transverse jet from top with a free surface.

Experimental investigation of a round jet using Digital Particle-Image Velocimetry (DPIV) was conducted by New et al [42]. Two shapes of jet were used; tophat jet and parabolic jet and the range of momentum ratio was 2.3 to 5.8 and the range of Reynolds number was 625-1645. They found that formation of leading-edge and lee-side vortices were significantly affected by the jet shape. In case of parabolic JICF (Fig 12), the shear layers were thicker than that of the tophat JICF (Fig 11) and thus take more time in vortex formation. In fact, in case of tophat JICF, the shear layers were thinner and large-scale vortices were formed readily and in a regular basis. So, for parabolic JICF, it is evident that it increases the jet penetration and decreases the near field entrainment of crossflow fluid. After measurement of streamwise and crossflow velocity components along the vertical planes at various locations downstream of the jet, they got a number of velocity maxima and minima. Their main consideration was the effect of jet geometries and entrainment of jet; however, it was conducted in a laminar flow and therefore no turbulence characteristics were reported.

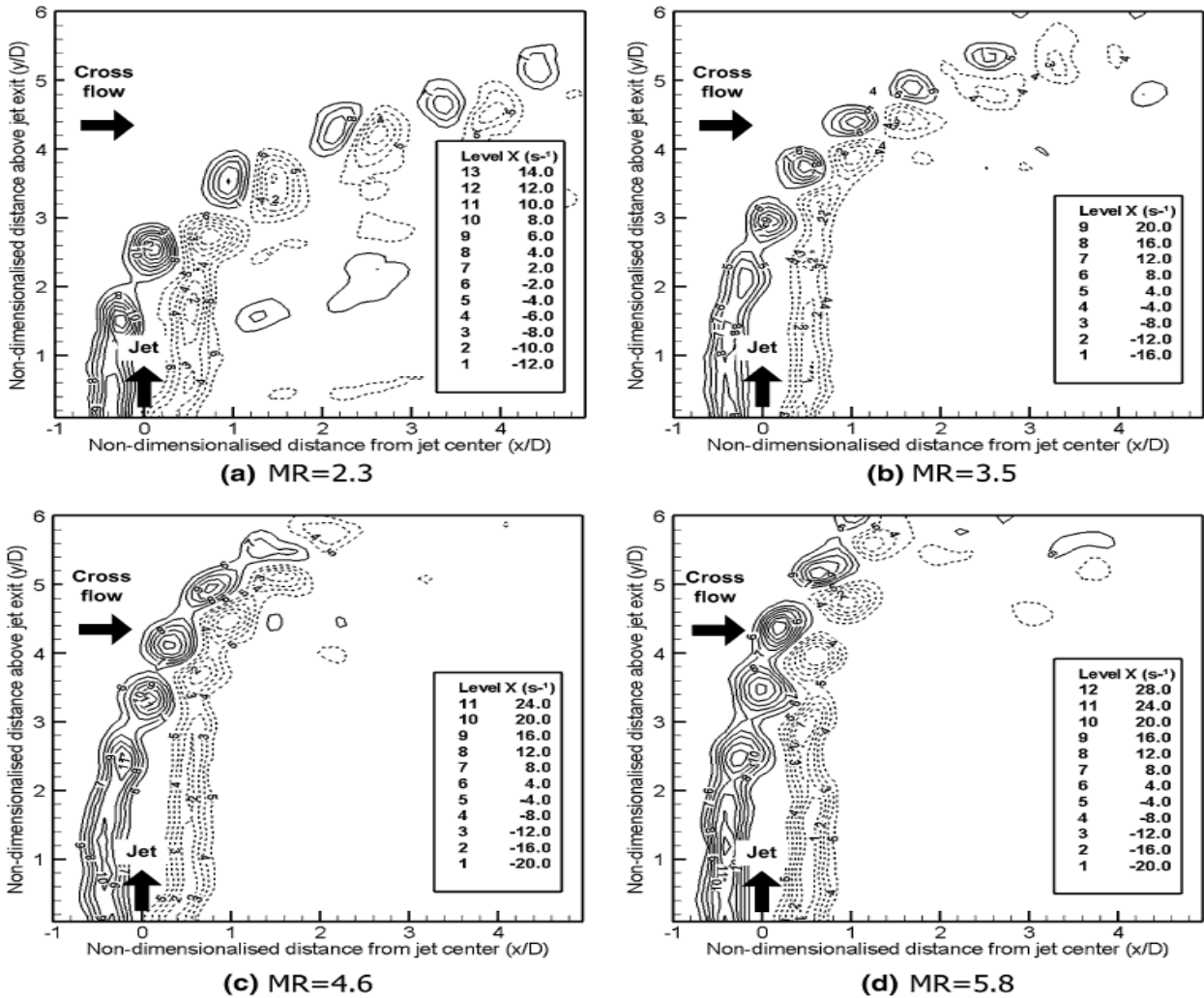


Fig 11 Instantaneous Velocity Fields along the Symmetry Plane for the Tophat JICF with MR =2.3 to 5.8 [42]



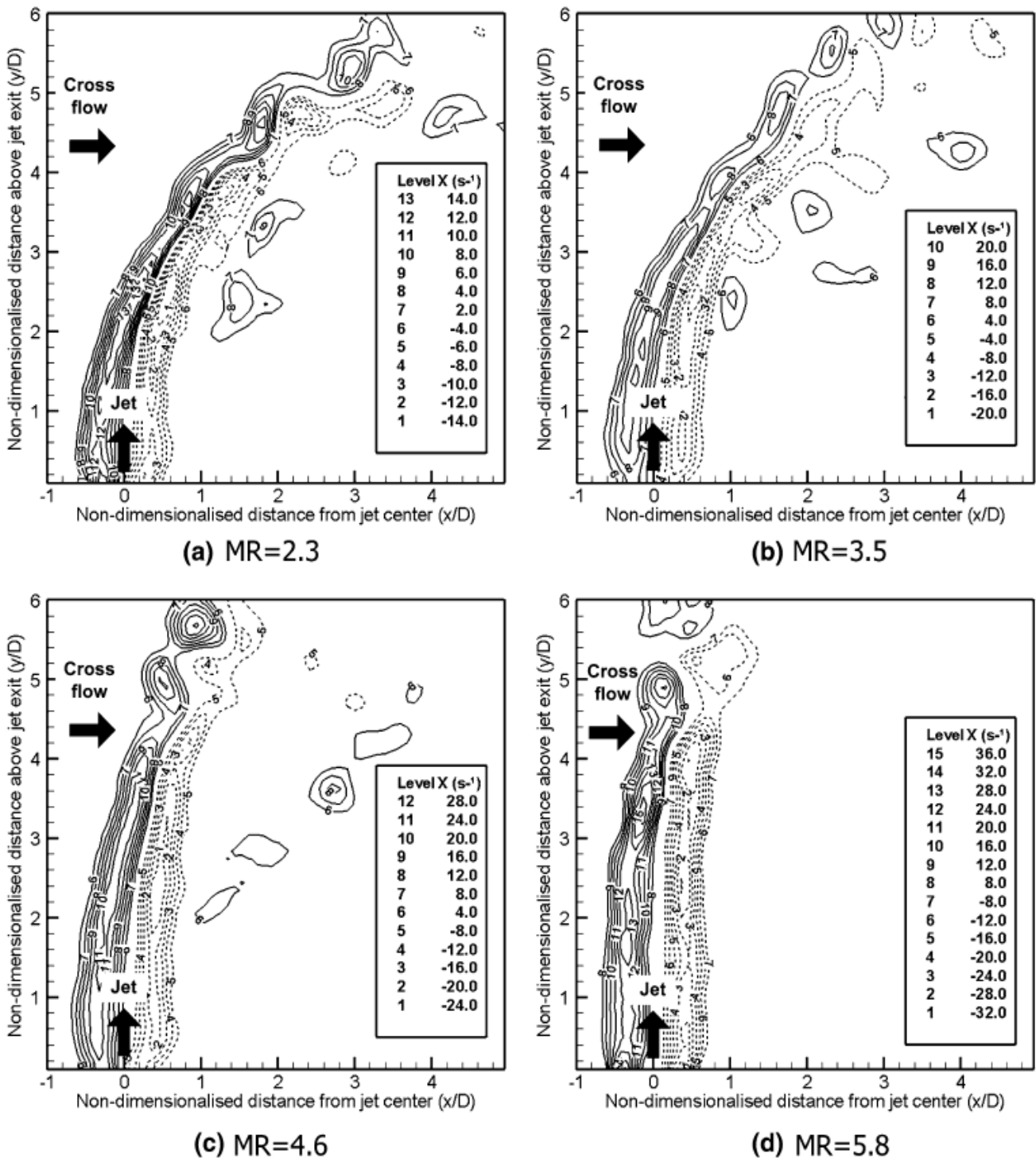


Fig 12 Instantaneous Velocity Fields along the Symmetry Plane for the Parabolic JICF with MR =2.3 to 5.8 [42]

A comparison between round turbulent jets and particle-laden jets in crossflow was studied by Diez et al [43]. The flow structures, issuing from a round turbulent single-phase jet and a particle laden jet with disperse phase, were considered and a time-resolved stereoscopic PIV (TR-ST-PIV) system was employed for the experimental procedure. The exit diameter of the jet was $d=3$ mm and jet Reynolds number was 13,500 with a velocity ratio of $r=18$. They found that the centreline jet penetration in vertical direction was greater for single phase turbulent jet than that of dispersed phase particle-laden jet which indicates that an increase in energy dissipation exists for the particle laden jets (Fig 13). In comparison with the end view (Fig 14), they

found a slight asymmetry in the region of vortices. The effect of the dispersed phase was not as noticeable as compared to side view velocity but the dispersed phase widens the region of mixing in both the transverse and vertical directions. All sets of experiments were carried out for a laminar crossflow with a turbulent jet flow. The flow behaviour in case of turbulent crossflow with a turbulent jet flow with small velocity ratio was not investigated.

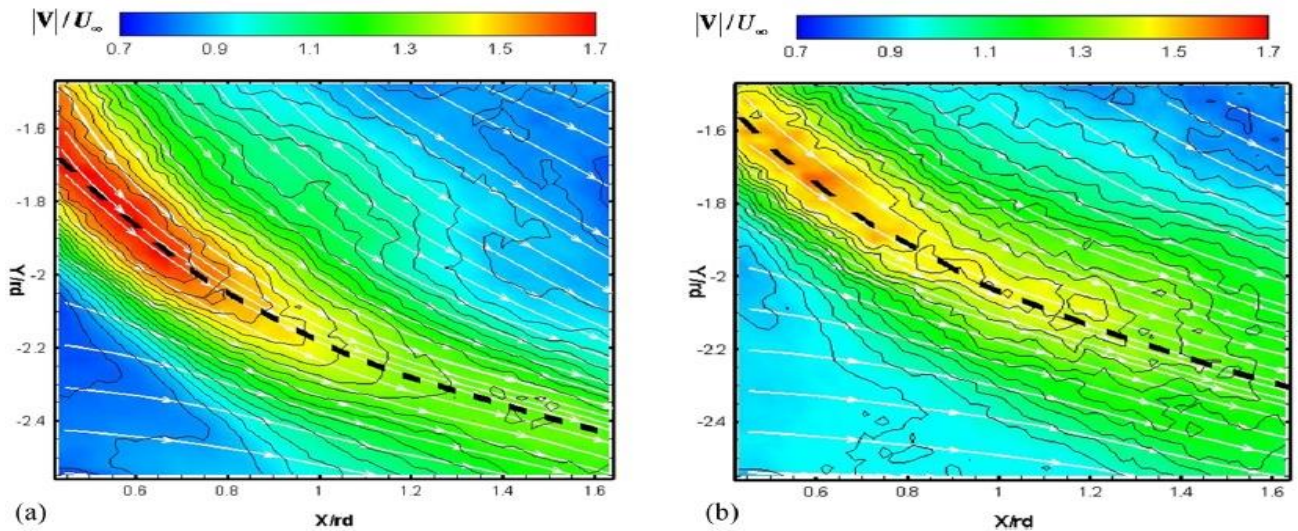


Fig 13 Contour plot of the mean velocity field, side view (a) for a jet and (b) for a particle-laden jet in crossflow. The streamlines are shown as solid white lines [43]

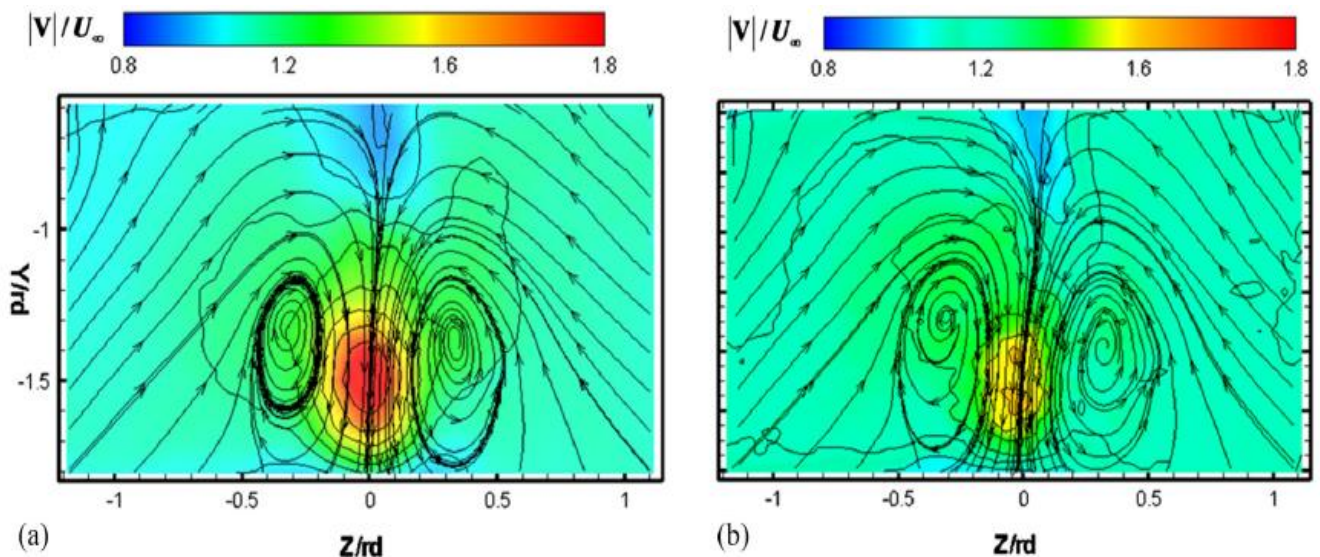


Fig 14 Contour plot of the mean velocity field, end view (a) for a jet and (b) for a particle-laden jet in crossflow. Streamlines are shown as solid black lines [43]

Experimental study by Cambonie et al [44] shows the significant effects of jet diameters in formation of counter rotating vortex pair (CVP). They conducted the experiment in a hydrodynamic channel and their flow was laminar. Volumetric Particle Tracking Velocimetry (VPTV) was used for flow visualization. They considered the range of velocity ratio from 0.5 to 3 and the range of boundary layer thickness was 1 to 2.5 cm. They focused on the influence of velocity ratio, boundary layer thickness and jet diameters in near and far field CVP. However, turbulence characteristics were not reported because of laminar flow (the range of Reynolds number was from 220 to 660).

Based on above literatures, for the jets issuing into crossflow from a channel bed, $r \leq 2-3$ is considered as low velocity ratio. Though there is no fixed range of low and high velocity ratio, but normally $r \geq 3$ is taken as high velocity ratio. For high velocity ratio, the centreline jet trajectory penetrates into the boundary layer and projects away from the wall (in the case where jet issues from the bottom). Due to the shear force effect, counter rotating

vortex forms and the flow behind the jet, in particular near the wall, becomes unsteady. This pattern of flow is similar to that of flow passes a solid cylinder. For low velocity ratio, on the other hand, the jet centreline remains close to the wall and it produces well defined wake structures. A water jet with a full 3D flow field with a low velocity ratio have not been studied and thus a detail investigation is needed to understand the flow structure of this kind of configuration.

IV. NUMERICAL STUDIES IN OPEN CHANNEL FLOW

Justification of low Reynolds number $k-\epsilon$ turbulence model was comprehensively studied by Hrenya et al [45]. For a fully developed pipe flow, numerical simulations were performed with four different Reynolds number. They considered models of ten researchers and compared their results. Table 2 shows those researchers' models with the numerical values of constants.

Table 2 Numerical Values of the Constants c_μ , c_1 , c_2 , σ_k and σ_ϵ

Researchers	Model	C_μ	C_1	C_2	σ_k	σ_ϵ
Jones and Launder (1972, 1973)	JL	0.09	1.45	2.0	1.0	1.3
Launder and Sharma (1974)	LS	0.09	1.44	1.92	1.0	1.3
Lam and Bremhorst (1981)	LB	0.09	1.44	1.92	1.0	1.3
Chien (1982)	CH	0.09	1.35	1.8	1.0	1.3
Lai and So (1990)	LSO	0.09	1.35	1.8	1.0	1.3
Myong and Kasagi (1990)	MK	0.09	1.4	1.8	1.4	1.3
So et al (1991)	SZS	0.096	1.5	1.83	0.75	1.45
Yang and Shih (1993)	YS	0.09	1.44	1.92	1.0	1.3
Fan et al (1993)	FLB	0.09	1.4	1.8	1.0	1.3
Rodi and Mansour (1993) and Michelassi et al (1993)	RMM	0.09	1.44	1.92	1.3	1.3

Experimental and numerical results were compared with different parameters like mean axial velocity, turbulent kinetic energy, eddy viscosity, Reynolds stress and turbulent dissipation rate. With different range of Reynolds numbers, those models provided significant qualitative and quantitative differences. They concluded that among all ten models, the Myong and Kasagi [46] model was best fit in predicting fully developed turbulent pipe flow. However, this model is poor for distribution of turbulent dissipation ϵ , and there is no evidence that this model will work for open channel.

Turbulent flow in an open channel (aspect ratio of $b/h=2$) with high Reynolds number was investigated by Shi et al [47]. They applied Large Eddy Simulation (LES) to see the effect of turbulence-driven secondary currents. LES code allows the free surface to deform freely so no special treatment for free-surface and wall damping functions were required. They obtained favourable agreement in comparison to the experimental results. However, for a channel with an aspect ratio of $b/h>5$ was not studied with this model. In addition, the computational time and cost was high in comparison to a two-equation model.

Modelling of three-dimensional velocity field in open channel flows was studied by Czernuszenko and Rylov [48]. They presented a simple model for calculation of three dimensional, stationary velocity field. They found that their model can calculate the stream wise velocity distribution as well as the secondary flow in a cross-section of regular channel. They considered tensor of turbulent shear stresses, mixing length tensor and tensor of turbulent normal stresses. The model was easy to calibrate by choosing the mixing length sizes. It allowed producing a relatively simple secondary flow structure as well as more complicated ones. The numerical procedure described by them was based on previously published data. Those data were concerned of the primary velocity distributions, the secondary currents patterns and the intensities of turbulence in the cross-section of the channel. Their main objective of the numerical simulations was to show how the model described the 3D velocity field in open channel flows for different structures of turbulence. They found that the formulae for mixing length and main components of mixing length ellipsoid

(MLE) were useful for open channel. However, defining the MLE is difficult in the cross-section of open channel, particularly in the corner of a channel.

Three dimensional numerical study of flows in open channel junctions was conducted by Huang et al [49]. They developed a new model for a junction flow and validated it with experimental data. The model was good for the junction flow, but it under predicts the effect of secondary currents; and secondary current is very common in open channel flow. In addition, there is no proof that this model is good for jet flow in an open channel.

Flow profile in a rectangular open channel was investigated by Gandhi et al [50] by using FLUENT. They validated their numerical model with experimental data taken by acoustic Doppler current profiler (ADCP). They found that for determining the optimum numbers and locations of flow sensors (for measurements of discharge in open channel), this proposed method is suitable. However, other parameters like turbulent intensity, shear stress, kinetic energy were not been presented in their studies.

Confluence flow in open channel was studied numerically by Yang et al [51]. They applied Dynamic meshes techniques and presented data in the form of water levels, longitudinal velocity and turbulent kinetic energy. All the coordinates were normalised with the width of the channel (Fig 15). Considering the distribution of longitudinal velocity they found that from the scale of separation point of view (positive velocity), realizable $k - \epsilon$ model shows the best agreement with the experimental data (Fig 16). However, from the magnitude of velocity point of view (the peak region, velocity <-1.4), the $k - \omega$ model shows best agreement among the three models (Fig 16). Considering the distribution of turbulent kinetic energy, the $k - \omega$ model shows good agreement (Fig 17). They compared different models for different parameter and concluded that there is no one “the best” model for all respects. This observation indicates the inapplicability of generalization of a single model for all the similar flow problems.



Review of Jets in a Cross Flow-Experimental and Numerical Approach

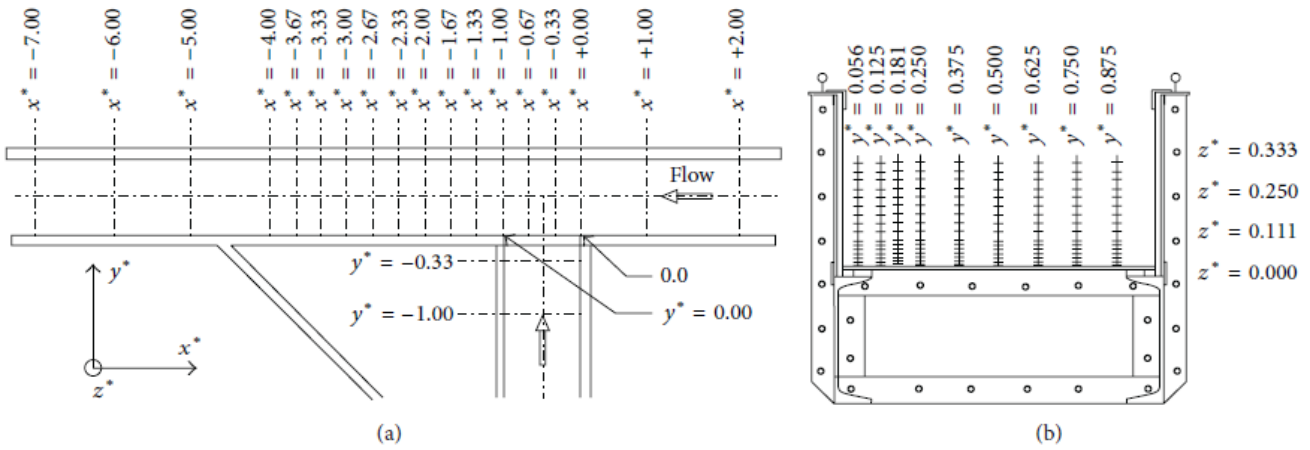


Fig 15 Measuring Points Arrangement in the Experiments [51]

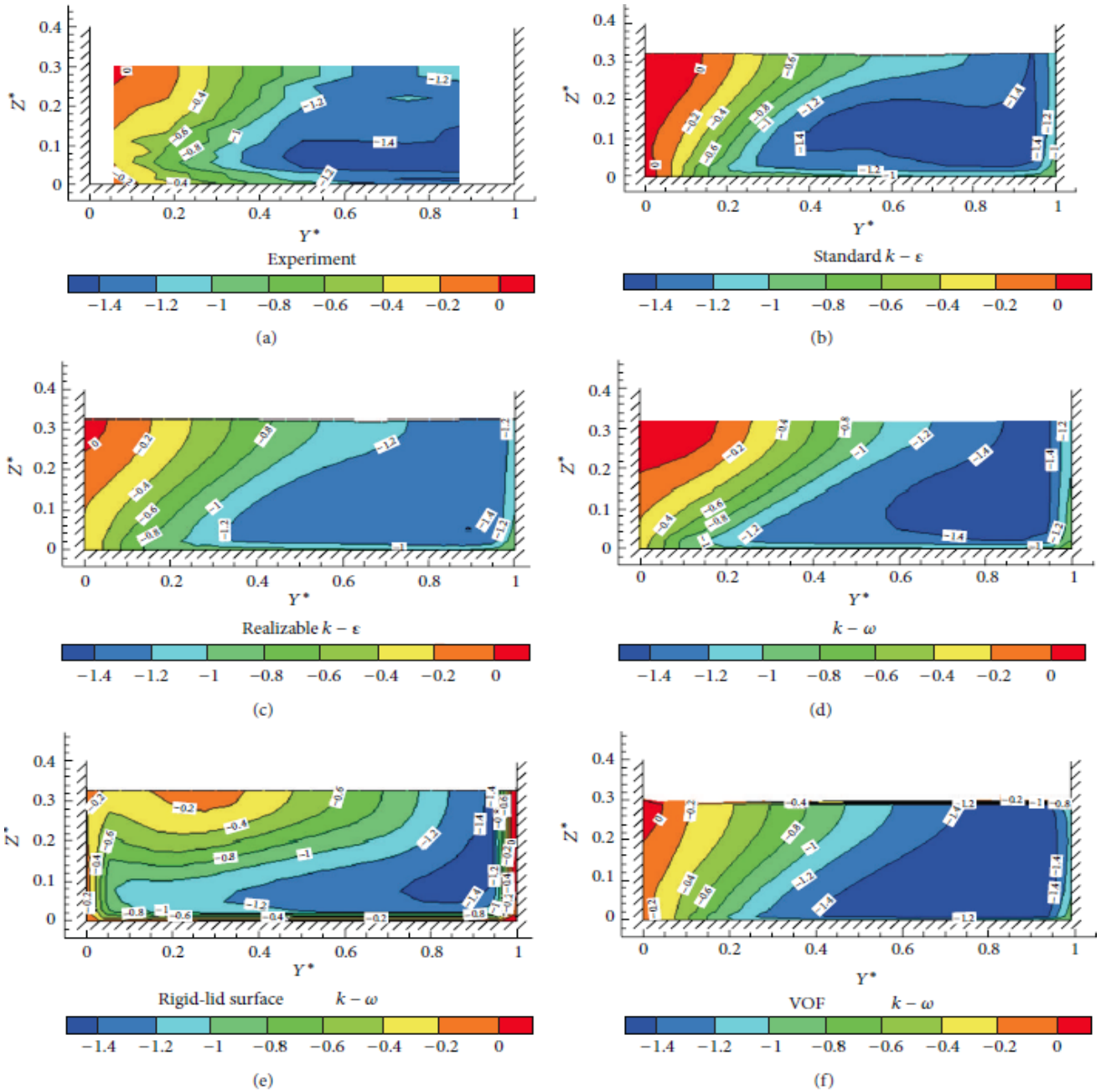


Fig 16 Contour of Longitudinal Velocity at $X^*=-3$ [51]

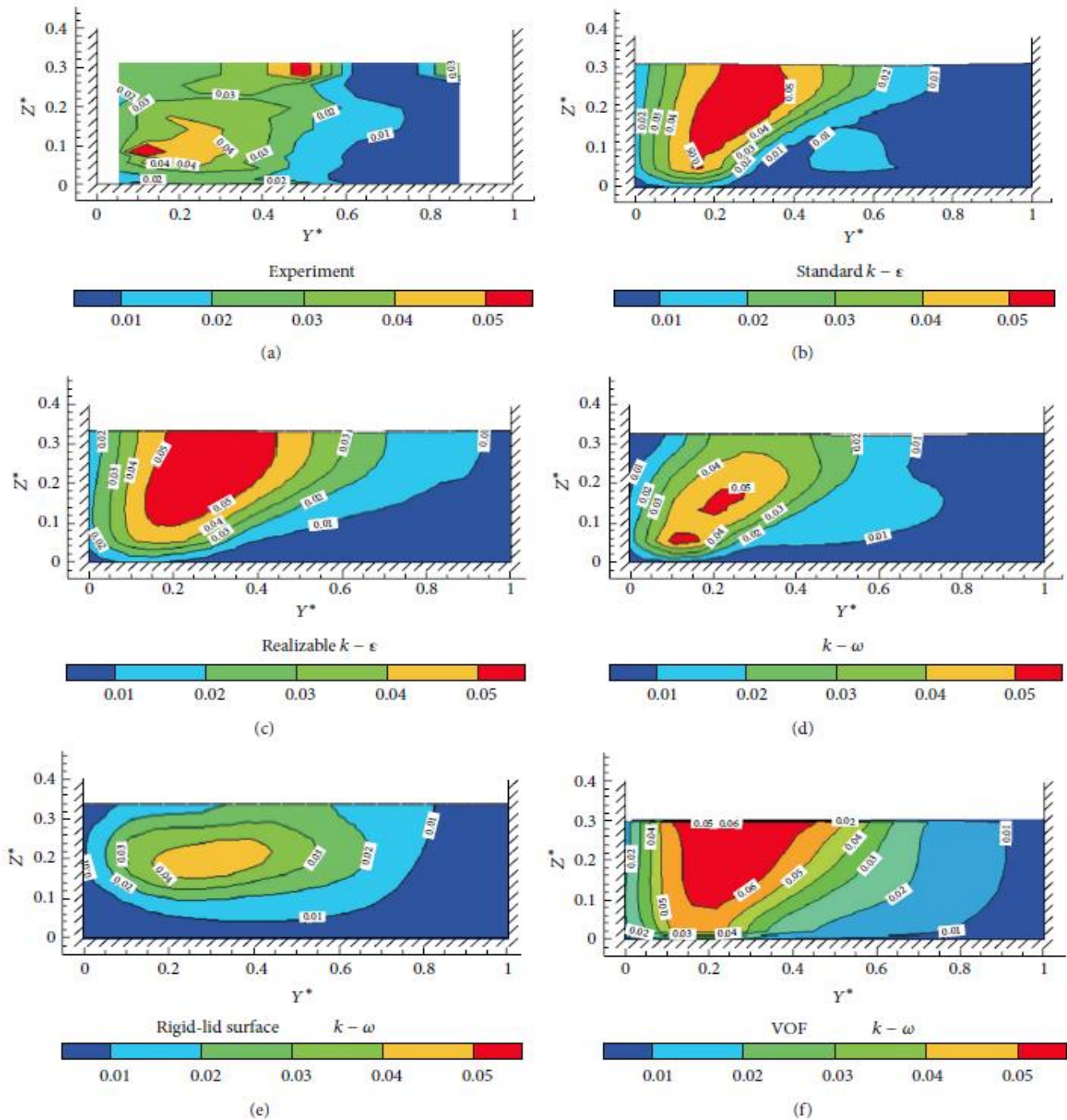


Fig 17 Contour of Turbulent Kinetic Energy At Cross Section $X^*=-3$ [51]

V. NUMERICAL STUDIES OF JETS IN CROSSFLOW

Investigation of slot jet issued into a crossflow was carried out by Jia et al [52]. Three turbulence models namely Shear Stress Transport (SST) $k - \omega$, V2F $k - \epsilon$ and RSM were employed to simulate the flow field. No damping function is needed for these models and the realizability constraints are fulfilled because of having a limiter on the time scales. The two equation SST $k - \omega$ model uses the modified version of turbulence viscosity and thus account for the transport of shear stress. This feature is an advantage over both the standard $k - \epsilon$ and $k - \omega$ model to perform better over these standard models.

The V2F is a four-equation model, where in addition to the k and ϵ , two more equations are solved; the velocity fluctuation normal to the streamlines $\overline{v'^2}$ and the transport

equation for the global relaxation factor. This effect avoids the need of damping functions. The most 'Physically sound' in RANS model is RSM and in this model Reynolds stresses are solved directly with the transport equation. Based on those three models, the researchers concluded that all the three models predict mean velocity reasonably well. However, the level of turbulence was under predicted by those models. Issuing a slot jet into a confined crossflow, a large recirculation zone was observed downstream of the jet because of the negative pressure gradient.

This phenomena is similar to the flow in a backward-facing step [53]. All these models predict the location and size of the recirculation zone, however, the predicted reattachment length were larger than the experiments. In addition, the RSM predicted unrealistic bulge around the reattachment point. This indicates that the RSM does not provide any superiority over the other two models. This results emphasis the uncertainty of selecting ‘the one’ turbulence model.

A CFD study of twin impinging jets in crossflow was done by Ostheimer and Yang [54]. They used both the RMS and $k - \epsilon$ model for better understanding of the complex flow field underneath of a V/STOL aircraft operating very close to the ground. A configuration of twin impinging jets along the span wise direction represents the flow field of this complex nature. They reproduced the pioneer research done by Barata et al [55] and employed both the RSM and $k - \epsilon$ model. They observed found that, for this particular flow field, RMS does not really show any superiority over the $k - \epsilon$ model. They recommended that LES is necessary to predict the second order turbulent quantities such as the shear and normal stresses more accurately.

Single circular jet exhausting from a flat plate into a crossflow was investigated by Chochua et al [56]. The standard $k - \epsilon$ turbulent model was employed to capture the flow field in terms of mean and root mean square (RMS) velocity distribution. They found that jet trajectory and jet mean exit velocity was captured reasonably well by this model but it over predicts the turbulent intensity at the jet exit. Numerical study of trajectories of jet in crossflow were presented by Muppidi and Mahesh [57]. They considered the jet flow which was issuing from bottom and Direct

Numerical Simulation (DNS) was used for simulation. They proposed a new length scale for describing the near field of the jet. They studied two different velocity ratios and found that jet trajectory depends on crossflow boundary layer thickness and the jet velocity profile. Turbulent jet in a laminar crossflow was investigated but the effect of turbulent jet in a laminar crossflow with DNS was not reported. In addition, free jet from top of the free surface for incompressible flow was not investigated using this model. Mechanism of jet mixing in a supersonic crossflow was studied by Kawai and Lele [58]. Unsteady supersonic jet mixing was investigated by numerical simulation and Large Eddy Simulation (LES) was performed. They analysed the structures of vortex formation in the mixing region because vortices play an important role in jet fluid stirring and subsequent mixing. In another study [59], they found that injection of a sonic jet into a supersonic turbulent crossflow produces vortices because of presence of pressure fluctuation inside the recirculation region. Pressure fluctuations are coupled with large-scale unsteady dynamics of jet injection into the injection area. They also observed the entrainment of the jet into the boundary layer separation bubble downstream of the jet injection (Fig 18). Mixing of jet fuel with the crossflow air inside a supersonic engine was considered in their experiment and the model showed good results in comparison with the experimental data. The model and results are based on the specific class of problem of jet mixing and do not give insight for incompressible flow particularly for the case of open channel with a crossflow.

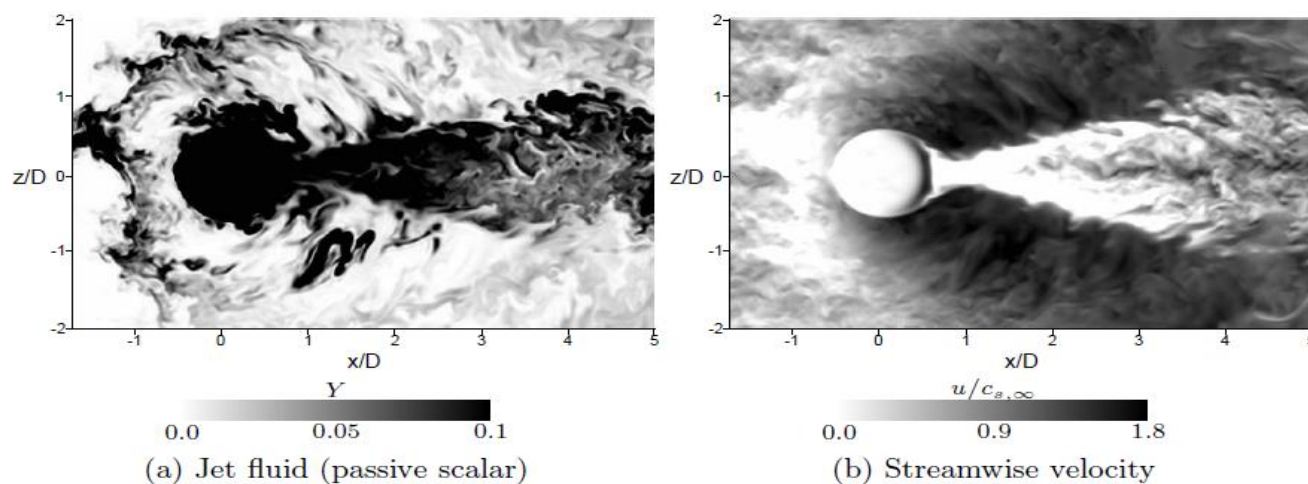


Fig 18 Jet Fluid Entrainment and Boundary Layer Separation Bubbles (a) Passive Scalar of Jet Fluid and (b) Stream Wise Velocity at Wall Parallel Plane Close to the Wall [59]

Different RANS based turbulence modelling techniques can be used for computations of turbulent flows [60]. In the case of non-swirling and impinging jets, Balabel and El-Askary [61] applied different $k - \epsilon$ based turbulence models. In their study, no surface heat transfer interaction was involved and they used both linear (standard, $v^2 - f$) and nonlinear (cubic) models. Since nonlinear models are very sensitive to the particular of the flow analysed, the results cannot be generalised, that indicates further investigation into the effects of different models on the accuracy of modelling. Jaramillo et al [62] numerically studied the performance and accuracy of different RANS-based turbulence models

(including algebraic stress models, both linear and non-linear eddy-viscosity models jointly with $k - \epsilon$ and $k - \omega$ models) and found that each model was only capable of capturing a particular flow region. In fact, models that shows good results for the case of round jet shows poor results in the plane jet configuration, indicating the sensitivity of the models to the particulars of the flow. Craft et al [63].

Studied the performance of different versions of $k - \varepsilon$ and Reynolds Stress Model (RMS). In their studies, for predicting the time-mean and time-resolved fluctuating quantities at the stagnation and wall jet regions, the RMS is found to be superior over the other models they have considered. But the study does not indicate whether it will be useful for transverse jet for an open channel case. For transitional regime (initially laminar or low turbulence jets), Angioletti et al [64] conducted the qualitative and quantitative comparisons between the computed flow behaviour and experimental results. They concluded that good predictions were achieved for velocity field with the RNG (Re-Normalization Group) $k - \varepsilon$ and RSM turbulence models but shows no generalized results for high turbulence jet. Pulat et al [65] reported significant improvement with standard $k - \varepsilon$ models when combined with a two-layer model of enhanced wall treatment.

VI. CONCLUSIONS

Experiments have significantly upgraded in sophistication over the past years. Pani and Dash [26], Sharp [66], Sarif and Pletcher [67], Larson and Jonsson [68], yoda [69], New et al [42], Yu et al [70] and many other researchers had done investigations and experiments with jet in crossflow. For estimating penetration and mixing, visualization still is an important component. Quantitative data are also necessary for that. Simulations have advanced from Reynolds-averaged methodology to large-eddy and hybrid methodologies. Considering low velocity ratio (jet to crossflow), experiments are less common and dispersion pattern with single jet in crossflow in water channel was not studied extensively. Quantitative data of velocity components and turbulent characteristics with low velocity jet are also less common. In addition, many of the previous methods of data collection were done using technology that were not advanced and this would surely impact the accuracy of the data set. A complete picture of a single jet issuing adversely in an open water channel (with fully developed boundary layer) was not studied fully and thus this flow field needs investigation both experimentally and numerically.

Symbols

b = Width of the channel
 C'^2 = Scalar variance
d = Diameter of nozzle
h = Depth of water
I = Turbulence intensity
k = Turbulence kinetic energy
L = Length of the channel
l = Length scale
 R_h = Hydraulic radius
 R_e = Reynolds number of crossflow
 R_{ej} = Reynolds number of jet
r = Velocity ratio ($\frac{u_j}{u_\infty}$)
s = Local maxima in the average velocity magnitude field
u = Mean velocity
 u_∞, u_{cross} = Velocity of crossflow
 u_j = Nozzle exit velocity
 $u' = \sqrt{u'^2}$ = Longitudinal velocity fluctuation

u'^2, v'^2 = Turbulent normal stresses
 u^* = Friction velocity
 $u' C'$ = Scalar flux components
 $\overline{u'v'}$ = Reynolds stress
 v, v, w = Mean velocity in x, y and z-direction
 $v' = \sqrt{v'^2}$ = Vertical velocity fluctuation
 x, y, z = Cartesian co-ordinate
 X^*, Y^*, Z^* = Normalised co-ordinates (normalised with the channel width)
 Δx_c = Grid resolution of the scalar field
 Δx_u = Grid resolution of the velocity fields
 y_{max} = Maximum height from the channel wall
 δ = Local mean flow width
 ε = Turbulence dissipation rate
 μ = Dynamic viscosity
 ν = Kinematic viscosity of water
 $\lambda_v \lambda_d$ = Length scale in velocity and scalar field
 σ_k = Turbulent Prandtl number for k
 σ_ε = Turbulent Prandtl number for ε
 τ = Shear stress
 ω = Specific dissipation rate

Abbreviation

ADCP = Acoustic Doppler current profiler
CFD = Computational fluid dynamics
CVP = Counter rotating vortex-pair
DNS = Direct numerical simulation
JICF = Jet in crossflow
LDA = Laser Doppler Anemometer
LDV = Laser Doppler Velocimeter
LES = Large eddy simulation
LIF = Laser Induced Fluorescence
MLE = Mixing length ellipsoid
PIV = Particle Image Velocimeter
RANS = Reynolds average Navier-Stokes
RMS = Root mean square
TKE = Turbulent kinetic energy
V/STOL = Vertical/Short take-off and landing
VPTV = Volumetric Particle Tracking Velocimetry

ACKNOWLEDGMENTS

The first author would like to acknowledge the scholarship received from the ECU-IPRS from the School of Engineering, Edith Cowan University.

REFERENCES

1. Sarma, K. V., Lakshminarayana, P., and Rao, N. L., Velocity distribution in smooth rectangular open channels. *Journal of Hydraulic Engineering*, 1983. 109: p. 270-289.
2. Nezu, I. and Rodi, W. Experimental study on secondary currents in open channel flow. in *Proceedings of 21st IAHR Congress*. 1985. Melbourne.
3. Tominaga, A., Nezu, I., Ezaki, K., and Nakagawa, H., Three-dimensional turbulent structure in straight open channel flows. *Journal of Hydraulic Research*, 1989. 27: p. 149-173.
4. Bonakdari, H., Larrarte, F., Lassabatere, L., and Joannis, C., Turbulent velocity profile in fully-developed open channel flows. *Environmental Fluid Mechanics*, 2008. 8: p. 1-17.



Review of Jets in a Cross Flow-Experimental and Numerical Approach

5. Yang, S. Q. and Lim, S. Y., Boundary shear stress distributions in smooth rectangular open channel flows. Proceedings of the ICE-Water Maritime and Energy, 1998. 130: p. 163-173.
6. Khodashenas, S. R., Abderrezzak, K. E. K., and Paquier, A., Boundary shear stress in open channel flow: A comparison among six methods. Journal of Hydraulic Research, 2008. 46: p. 598-609.
7. Margason, R. J. Fifty years of jet in cross flow research. In AGARD, Computational and Experimental Assessment of Jets in Cross Flow 41 p (SEE N94-28003 07-34). 1993.
8. Kamotani, Y. and Greber, I., Experiments on a turbulent jet in a cross flow. AIAA journal, 1972. 10: p. 1425-1429.
9. Andreopoulos, J. and Rodi, W., Experimental investigation of jets in a crossflow. J. Fluid Mech, 1984. 138: p. 93-127.
10. Fric, T. and Roshko, A., Vortical structure in the wake of a transverse jet. Journal of Fluid Mechanics, 1994. 279: p. 1-47.
11. Kelso, R. M., Lim, T., and Perry, A. E., An experimental study of round jets in cross-flow. Journal of Fluid Mechanics, 1996. 306: p. 111-144.
12. Megerian, S., Davitian, J., de B Alves, L., and Karagozian, A., Transverse-jet shear-layer instabilities. Part I. Experimental studies. Journal of Fluid Mechanics, 2007. 593: p. 93-129.
13. Smith, S. and Mungal, M., Mixing, structure and scaling of the jet in crossflow. Journal of Fluid Mechanics, 1998. 357: p. 83-122.
14. Su, L. and Mungal, M., Simultaneous measurements of scalar and velocity field evolution in turbulent crossflowing jets. Journal of Fluid Mechanics, 2004. 513: p. 1-45.
15. Shan, J. W. and Dimotakis, P. E., Reynolds-number effects and anisotropy in transverse-jet mixing. Journal of Fluid Mechanics, 2006. 566: p. 47-96.
16. Sherif, S. and Pletcher, R., Measurements of the flow and turbulence characteristics of round jets in crossflow. Journal of fluids engineering, 1989. 111: p. 165-171.
17. de B Alves, L. S., Kelly, R. E., and Karagozian, A. R., Transverse-jet shear-layer instabilities. Part 2. Linear analysis for large jet-to-crossflow velocity ratio. Journal of Fluid Mechanics, 2008. 602: p. 383-401.
18. Muppidi, S. and Mahesh, K., Direct numerical simulation of round turbulent jets in crossflow. Journal of Fluid Mechanics, 2007. 574: p. 59-84.
19. Herrmann, M., Detailed numerical simulations of the primary atomization of a turbulent liquid jet in crossflow. Journal of Engineering for Gas Turbines and Power, 2010. 132: p. 061506.
20. Steffler, P. M., Rajaratnam, N., and Peterson, A. W., LDA measurements in open channel. Journal of Hydraulic Engineering, 1985. 111: p. 119-130.
21. Nezu, I. and Rodi, W., Open-channel flow measurements with a laser Doppler anemometer. Journal of Hydraulic Engineering, 1986. 112: p. 335-355.
22. Nezu, I., Turbulence in open-channel flows. 1993.
23. Guo, J. and Julien, P. Y., Shear stress in smooth rectangular open-channel flows. Journal of hydraulic engineering, 2005. 131: p. 30-37.
24. Blanckaert, K., Buschman, F., Schielen, R., and Wijnnga, J., Redistribution of velocity and bed-shear stress in straight and curved open channels by means of a bubble screen: Laboratory experiments. Journal of hydraulic engineering, 2008. 134: p. 184-195.
25. Cebeci, T., Turbulence models and their application: efficient numerical methods with computer programs. 2004: Springer Science & Business Media.
26. Pani, B. and Dash, R., Three-dimensional single and multiple free jets. Journal of Hydraulic Engineering, 1983. 109: p. 254-269.
27. Andreopoulos, J., On the structure of jets in a crossflow. Journal of Fluid Mechanics, 1985. 157: p. 163-197.
28. Morton, B. R. and Ibbetson, A., Jets deflected in a crossflow. Experimental Thermal and Fluid Science, 1996. 12: p. 112-133.
29. Lim, T., New, T., and Luo, S., On the development of large-scale structures of a jet normal to a cross flow. Physics of Fluids (1994-present), 2001. 13: p. 770-775.
30. Coelho, S. L. and Hunt, J., The dynamics of the near field of strong jets in crossflows. Journal of Fluid Mechanics, 1989. 200: p. 95-120.
31. Getsinger, D. R., Hendrickson, C., and Karagozian, A. R., Shear layer instabilities in low-density transverse jets. Experiments in Fluids, 2012. 53: p. 783-801.
32. Blanchard, J., Brunet, Y., and Merlen, A., Influence of a counter rotating vortex pair on the stability of a jet in a cross flow: an experimental study by flow visualizations. Experiments in fluids, 1999. 26: p. 63-74.
33. Oktay, O. and Larsen, P. S., Laser Doppler anemometry study of a turbulent jet in crossflow. AIAA journal, 2003. 41: p. 1614-1616.
34. Roth, K. R., Fearn, R. L., and Thakur, S. S., Evaluation of a Navier-Stokes Prediction of a Jet in a Crossflow. Journal of aircraft, 1992. 29: p. 185-193.
35. Eroglu, A. and Breidenthal, R. E., Exponentially accelerating jet in crossflow. AIAA journal, 1998. 36: p. 1002-1009.
36. Gyr, A. and Kinzelbach, W., Sedimentation and sediment transport. 2003: Springer.
37. Camussi, R., Guj, G., and Stella, A., Experimental study of a jet in a crossflow at very low Reynolds number. Journal of Fluid Mechanics, 2002. 454: p. 113-144.
38. Barata, J. and Duro, D., Laser-Doppler measurements of impinging jet flows through a crossflow. Experiments in fluids, 2004. 36: p. 665-674.
39. Barata, J. M., Carvalho, P. S., Neves, F. M., Silva, A. R., Vieira, D. F., and Durão, D. F., Laser Doppler Measurements of Twin Impinging Jets Aligned with a Crossflow. Journal of Physical Science and Application, 2014. 4: p. 403-411.
40. Gopalan, S., Abraham, B. M., and Katz, J., The structure of a jet in cross flow at low velocity ratios. Physics of fluids, 2004. 16: p. 2067.
41. White, F. M., Viscous fluid flow. Vol. 46. 2006: McGraw-Hill Higher Education Boston.
42. New, T., Lim, T., and Luo, S., Effects of jet velocity profiles on a round jet in cross-flow. Experiments in fluids, 2006. 40: p. 859-875.
43. Diez, F., Torregrosa, M., and Pothos, S., A comparison between round turbulent jets and particle-laden jets in crossflow by using time-resolved stereoscopic particle image velocimetry. Journal of Fluids Engineering, 2011. 133: p. 091301.
44. Cambonie, T., Gautier, N., and Aider, J.-L., Experimental study of counter-rotating vortex pair trajectories induced by a round jet in cross-flow at low velocity ratios. Experiments in fluids, 2013. 54: p. 1-13.
45. Hrenya, C., Bolio, E., Chakrabarti, D., and Sinclair, J., Comparison of low Reynolds number $k-\epsilon$ turbulence models in predicting fully developed pipe flow. Chemical Engineering Science, 1995. 50: p. 1923-1941.
46. Myong, H. K. and Kasagi, N., A new approach to the improvement of $k-\epsilon$ turbulence model for wall-bounded shear flows. JSME International Journal, 1990. 33: p. 63-72.
47. Shi, J., Thomas, T., and Williams, J., Large-eddy simulation of flow in a rectangular open channel. Journal of Hydraulic Research, 1999. 37: p. 345-361.
48. Czernuszkeno, W. and Rylov, A., Modeling of three-dimensional velocity field in open channel flows. Journal of Hydraulic Research, 2002. 40: p. 135-143.
49. Huang, J., Weber, L. J., and Lai, Y. G., Three-dimensional numerical study of flows in open-channel junctions. Journal of hydraulic engineering, 2002. 128: p. 268-280.
50. Gandhi, B., Verma, H., and Abraham, B. Investigation of Flow Profile in Open Channels using CFD. in Proc. 8th Intl. Conference on Hydraulic Efficiency Measurement. 2010.
51. Yang, Q., Liu, T., Lu, W., and Wang, X., Numerical Simulation of Confluence Flow in Open Channel with Dynamic Meshes Techniques. Advances in Mechanical Engineering, 2013. 2013.
52. Jia, R., Sundén, B., Miron, P., and Léger, B., A numerical and experimental investigation of the slot film-cooling jet with various angles. Journal of turbomachinery, 2005. 127: p. 635-645.
53. Jayaraj, S., Saleel, C., and Shaija, A., On Simulation of Backward Facing Step Flow Using Immersed Boundary Method. International Journal of Advanced Computer Science, 2013. 3.
54. Ostheimer, D. and Yang, Z., A CFD Study of Twin Impinging Jets in a Cross-Flow. The Open Numerical Methods Journal, 2012. 4: p. 24-34.
55. Barata, J., Duro, D., Heitor, M., and McGuirk, J., The turbulence characteristics of a single impinging jet through a crossflow. Experimental thermal and fluid science, 1992. 5: p. 487-498.
56. Chochua, G., Shyy, W., Thakur, S., Brankovic, A., Lienau, J., Porter, L., and Lischinsky, D., A computational and experimental investigation of turbulent jet and crossflow interaction. Numerical Heat Transfer: Part A: Applications, 2000. 38: p. 557-572.
57. Muppidi, S. and Mahesh, K., Study of trajectories of jets in crossflow using direct numerical simulations. Journal of Fluid Mechanics, 2005. 530: p. 81-100.
58. Kawai, S. and Lele, S. K., Mechanisms of jet mixing in a supersonic crossflow: a study using large-eddy simulation. AIAA paper, 2008. 4575: p. 2008.

59. Kawai, S. and Lele, S., Dynamics and mixing of a sonic jet in a supersonic turbulent crossflow. Center for Turbulence Research Annual Research Briefs, 2009: p. 285-298.
60. Nallasamy, M., Turbulence models and their applications to the prediction of internal flows: a review. Computers & Fluids, 1987. 15: p. 151-194.
61. Balabel, A. and El-Askary, W., On the performance of linear and nonlinear $k-\epsilon$ turbulence models in various jet flow applications. European Journal of Mechanics-B/Fluids, 2011. 30: p. 325-340.
62. Jaramillo, J., Perez-Segarra, C., Rodriguez, I., and Oliva, A., Numerical study of plane and round impinging jets using RANS models. Numerical Heat Transfer, Part B: Fundamentals, 2008. 54: p. 213-237.
63. Craft, T., Graham, L., and Launder, B. E., Impinging jet studies for turbulence model assessment—II. An examination of the performance of four turbulence models. International Journal of Heat and Mass Transfer, 1993. 36: p. 2685-2697.
64. Angioletti, M., Nino, E., and Ruocco, G., CFD turbulent modelling of jet impingement and its validation by particle image velocimetry and mass transfer measurements. International Journal of Thermal Sciences, 2005. 44: p. 349-356.
65. Pulat, E., Isman, M. K., Etemoglu, A. B., and Can, M., Effect of turbulence models and near-wall modeling approaches on numerical results in impingement heat transfer. Numerical Heat Transfer, Part B: Fundamentals, 2011. 60: p. 486-519.
66. Sharp, J., Effect of waves on buoyant jets. Institution of Civil Engineers Proceedings pt. 2, 1986. 81: p. 471-475.
67. Sherif, S. and Pletcher, R. Measurements of the flow and turbulence characteristics of round jets in cross flow. in 4th Fluid Mechanics, Plasma Dynamics and Lasers Conference. 1986.
68. Larson, M. and Jonsson, L., Modeling of mixing by turbulent jet in stably stratified fluid. International Journal of Multiphase Flow, 1996. 22: p. 131-132.
69. Yoda, M. and Fiedler, H., The round jet in a uniform counterflow: flow visualization and mean concentration measurements. Experiments in fluids, 1996. 21: p. 427-436.
70. Yu, D., Ali, M., and Lee, J. H., Multiple tandem jets in cross-flow. Journal of Hydraulic Engineering, 2006. 132: p. 971-982.